Oxygen isotope analysis in garnet by ion microprobe: new insights from high-precision analyses..a preliminary look

F. Zeb Page[1], Noriko T. Kita[2], and John W. Valley[2]

[1]Department of Geology, Oberlin College, Oberlin, OH; [2], Department of Geology & Geophysics, University of Wisconsin - Madison

Standards, Reproducibility and Calibration

The newest generation of ion microprobes allows unprecedented precision in stable isotope analyses at very small scales. Although the matrix effects of cation solid solution on Instrument Mass Fractionation (IMF) have been a subject of study for some time (e.g., Eiler et al., 1997; Riciputi et al., 1998) there is as yet little published on matrix effects in large-radius multicollector ion probes. Vielzeuf et al. (2005) began this work on Al-rich garnets, but, advances in precision made only in the last few years warrants the reexamination of standards and methods. The current study evaluates the same commonly available Al-rich garnet standards as well as additional standards that are both Al and Fe^{3+}-rich. A strong correlation is found between estimated molar volume and IMF and is applied as a new correction scheme.

Table 1. Cation composition, IMF relative to the UWG-2 standard and analytical stability over time of garnet standards. All garnet standards are corrected with a primary standard (UWG-2) in order to deconvolute the different issues of instrument stability and matrix effects.

	mole %										Reproducibility over time (IMF relative to UWG-2)									
Standard	Alm	Pyp	Sps	Grs	Andr	Uvar	CaTi grt	calculated molar V	1σ	SIMS 1σ	4.2006	8.2006	9.2006	11.2006	1.2007	4.2007	6.2007	Average	1σ	Range	Laser $\delta^{18}O$
Pyrope $Mg_3Al_2Si_3O_{12}$																					
PypDM	2.79	96.72	0.06	0.42	0.01	0.00	0.00	113.2	0.03	0.29	-1.5	-1.1			-0.9	-0.8		-1.1	0.3	0.7	5.60
PypAA	17.83	68.92	0.77	11.70	0.00	0.73	0.04	115.1	0.1	0.13	-0.3							-0.3			5.50
13-63-19	17.98	71.36	0.77	9.37	0.33	0.18	0.01	114.8	0.02	0.15	-0.2							-0.2			5.92
PypAK	23.70	63.63	0.79	11.44	0.00	0.42	0.03	115.1	0.04	0.21	-0.3							-0.3			5.50
PypMM	25.45	62.78	0.78	10.55	0.16	0.00	0.28	115.1	0.11	0.30	0.3							0.3			5.30
13-62-29	32.33	58.94	0.92	7.49	0.20	0.04	0.09	114.8	0.01	0.28	-0.5							-0.5			7.39
13-63-20	30.54	47.63	0.60	20.66	0.40	0.02	0.15	116.4	0.06	0.17	0.7							0.7			6.14
13-63-44	29.34	44.33	0.64	25.27	0.23	0.05	0.14	117.0	0.03	0.27	0.7							0.7			6.37
13-62-27	34.51	48.85	0.74	15.51	0.21	0.06	0.11	115.9	0.02	0.18	0.2							0.2			6.49
Almandine $Fe_3Al_2Si_3O_{12}$																					
UWG-2	45.44	39.91	0.91	13.71	0.00	0.00	0.02	115.8	0.03	0.16	0.0							0.0			5.80
Bal509	51.68	44.38	0.59	3.25	0.10	0.00	0.00	114.7	0.79	0.15	-1.0							-1.0			12.30
13-63-21	41.45	25.70	0.69	31.36	0.43	0.01	0.36	118.1	0.03	0.13	1.3		1.3					1.3	0.0	0.0	4.55
Beta114	61.58	30.83	1.57	5.80	0.21	0.00	0.00	115.3	0.49	0.27	-0.9		-0.7	-0.7	-0.5			-0.7	0.2	0.4	9.30
AlmCMG	69.99	24.63	2.43	2.90	0.05	0.00	0.00	115.1	0.17	0.32	-0.5							-0.5			7.50
AlmSE	73.43	25.24	0.37	0.92	0.05	0.00	0.00	114.9	0.02	0.14	-1.2	-1.1	-1.2	-1.0	-1.2			-1.1	0.1	0.2	8.30
2B3	66.84	2.97	4.04	24.03	2.08	0.01	0.03	118.1	1.96	0.22	1.1	1.1	1.0		1.0			1.1	0.1	0.2	6.90
Spessartine $Mn_3Al_2Si_3O_{12}$																					
SpeSE	5.70	0.05	94.04	0.21	0.00	0.00	0.00	116.9	0.01	0.21	-0.7	-0.6			-0.6			-0.6	0.1	0.1	5.40
Grossular $Ca_3Al_2Si_3O_{12}$																					
R-53	18.66	19.19	0.29	61.04	0.00	0.03	0.79	121.2	0.07	0.14	2.4	2.5						2.4	0.1	0.2	5.33
GrsSE	2.73	0.05	1.44	94.45	0.22	0.04	1.07	125.1	0.04	0.17	2.7	2.8	2.9		2.8	3.2		2.9	0.2	0.5	3.80
MexGrs	1.36	2.54	0.98	85.63	8.45	0.01	1.02	125.5	0.35	0.31	5.6						5.5	5.5	0.1		10.60
Andradite $Ca_3Fe^{3+}_2Si_3O_{12}$																					
92LEW8	4.05	0.83	0.39	43.37	48.72	0.05	2.61	128.4	1.98	0.32	5.4							5.4		0.0	-0.93
92LEW10	4.48	0.56	0.35	42.28	50.21	0.01	2.10	128.4	2.07	0.21	5.6						5.7	5.7	0.1	0.0	-1.20
92LEW7	3.50	0.17	0.18	6.49	89.44	0.04	0.17	131.0	1.34	0.13	6.7						6.6	6.7	0.1		-1.60
92LEW2	2.95	0.12	0.18	5.56	91.08	0.04	0.06	131.1	1.49	0.39	7.1							7.1			-1.47

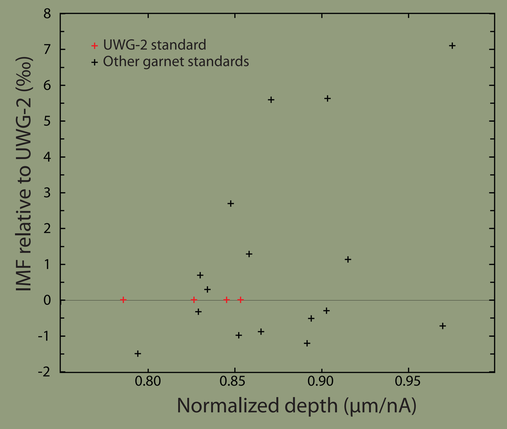

Figure 1. It has been proposed that IMF may be caused by differential sputtering rates (Eiler et al., 1997). In order to evaluate this, a sputter test was conducted using the WiscSIMS IMS-1280 in a 10x10µm raster mode. Pit depths were measured with a Zygo white-light profilometer and normalized to the average primary current during sputtering. No correlation is observed between pit-depth and IMF.

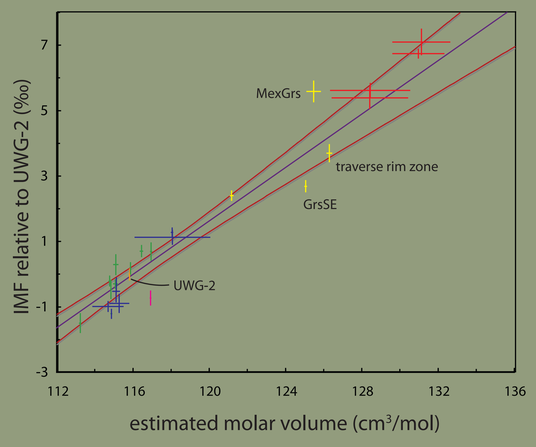

Figure 2. Correlation between IMF and estimated molar volume (as a function of cation composition) Standards are color coded according to the dominant garnet end-member as in Table 1. Error bars are 2σ. Large errors for andradite-rich garnets are due in part to estimation of Fe^{3+} by EPMA. Scatter around this correlation line is greater than analytical error, and is most pronounced among the grossular-rich standards.

An Application

Hydrothermal garnets from the Adirondack Mts. have oscillatory zoning in both cations and oxygen isotopes that were preserved through granulite-facies metamorphism (Clechenko & Valley, 2003). One of these well-characterized garnets was chosen as a test for oxygen analyses by ion probe in garnet.

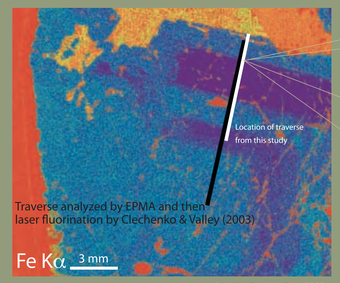

Clechenko & Valley (2003)

Figure 3. X-ray map of a metamorphosed skarn garnet from Clechenko & Valley (2003) showing oscillating bands of Fe^{3+}-rich andradite and Al-rich grossular garnet. The black line shows the traverse made by Clechenko & Valley using first EPMA and then a thin saw-blade + laser fluorination technique for $\delta^{18}O$. The white line indicates the EPMA and ion probe traverse in the present study.

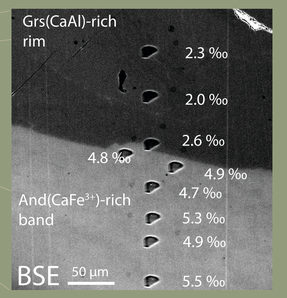

Figure 4. Back-scattered electron (BSE) image of ion-probe pits across the boundary between a high-$\delta^{18}O$, Fe^{3+}-rich band and a low $\delta^{18}O$, Al-rich band. $\delta^{18}O$ values are corrected as in Figure 6, and are appoximate.

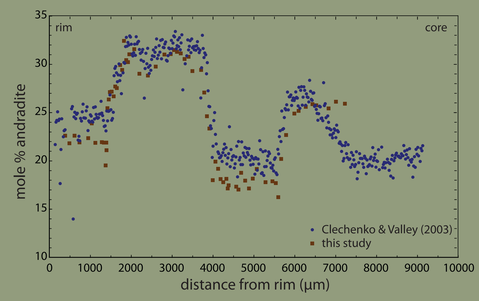

Figure 5. EPMA traverses of the same garnet showing the mole % andradite ($Ca_3Fe^{3+}_2Si_3O_{12}$) from this study and that of Clechenko & Valley (2003). The EMPA data from this study have been shifted 360 µm away from rim in order to better match the data from the 2003 study. The same correction has been made to the ion probe analyses in Figure 6. The mol % andradite in this study are systematically lower than that of Clechenko & Valley (2003) probably due to a different method of estimating Fe^{3+}.

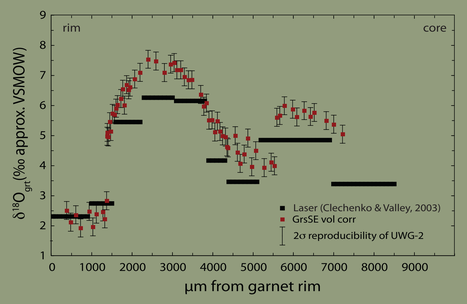

Figure 6. $\delta^{18}O$ traverses of the skarn garnet. Ion probe data was corrected for IMF using a molar volume correction bewteen two andradite standards (92LEW10 and 92LEW7) and the grossular standard GrsSE. Based on the mismatch of the two traverses for high-andradite zones, this correction appears to under-correct high Fe^{3+} garnet by up to ~1‰. Corrections using MexGrs instead of GrsSE are shifted down ~ 2‰. If the data are corrected using the laser data for the outermost rim of the traverse, results are similar to those shown. The ion probe data appear to show diffusion of oxygen across the relatively sharp cation boundary shown in Figure 4.

Significant variability in IMF among well-characterized garnet standards of similar cation composition appears to be that largest obstacle to high-precision oxygen isotope analyses of garnet. This variablilty is present throughout the compositional spectrum of garnets, but is most pronounced between grossular standards in the current standard set.

As observed by Vielzeuf et al. (2005) calcium garnet appears to have the largest effect on IMF. New data on andradite garnet shows that it has an even larger effect on IMF than grossular, and that this scales with molar volume. Correction schemes based on molar volume appear to have promise, but are hampered by variability in standards in the same way as compositional bracketing methods such as that of Vielzeuf et al. (2005).

References

Clechenko, C.C. and Valley, J.W., 2003. Oscillatory zoning in garnet from the Willsboro wollastonite skarn, Adirondack Mts, New York: a record of shallow hydrothermal processes preserved in a granulite facies terrane. J. Metam. Geol., 21: 771-784.

Eiler, J.M., Graham, C.M. and Valley, J.W., 1997. SIMS analysis of oxygen isotopes; matrix effects in complex minerals and glasses. Chem. Geol., 138: 221-244.

Riciputi, L.R., Paterson, B.A. and Ripperdan, R.L., 1998. Measurement of light stable isotope ratios by SIMS:: Matrix effects for oxygen, carbon, and sulfur isotopes in minerals. International Journal of Mass Spectrometry, 178: 81-112

Vielzeuf, D., Champenois, M., Valley, J.W., Brunet, F. and Devidal, J.L., 2005. SIMS analyses of oxygen isotopes: Matrix effects in Fe-Mg-Ca garnets. Chem. Geol., 223: 208-226.